Revivals and superstructures in the Jaynes-Cummings model with a small number of photons

P. F. Góra and C. Jedrzejek
Institute of Physics, Jagellonian University, Reymonta 4, 30-059 Kraków, Poland
(Received 11 June 1993)

If the quantized field has initially a small mean number of photons ($\bar{n} \sim 2$), quantum inversion displays distinct revivals, provided the detuning between the field and the atom is large as compared to the coupling constant [$(g/\Delta)^2 \ll 1$]. However, the amplitudes of these revivals are very small. For long times, individual revivals partially overlap to form fractional revivals, and for even longer times superrevivals (revivals of the revivals) appear. These phenomena result from the beating of modes of the quantized field that are not nearest neighbors. The envelope of the electric field associated with the oscillating atomic dipole exhibits similar superstructures, but with a period twice that for the atomic inversion.

PACS number(s): 42.50.Md, 32.90.+a

I. INTRODUCTION

The Jaynes-Cummings (JC) model [1] of a two-level atom interacting with a single mode of electromagnetic radiation has been attracting interest as one of the few models which can be solved exactly and give nontrivial results, and this interest was further enhanced when progress in experimental techniques involving Rydberg atoms and high-Q cavities made it possible to observe "practically two-level" atoms in the laboratory [2]. Using these techniques it is in principle possible to build a single-atom maser [3], and the interaction between a single atom and its own radiation field has been observed for the first time by Rempe, Walther, and Klein [4]. Periodical collapses and revivals of the initial atomic population [5] form the most spectacular feature of the Jaynes-Cummings model. These quantum revivals have been first described for a case of an initially coherent state of the field. They result from beating of all modes of the quantized field. However, as an overall phase difference between these modes accumulates, revivals start to overlap and then they vanish altogether.

Many authors have also been investigating the JC model with a different initial state of the field and/or the atom. In particular, some unexpected long-time behavior of the atomic inversion has been reported for an initially sub-Poissonian statistics of the field [6]. The long-time behavior of the model is governed by the fractional-revival scenario: at certain times revivals follow each other two, three, four, etc., times faster than the original ones. These fractional revivals are associated with the field splitting into combinations of macroscopically distinguishable states. As we have shown in our previous work [7], these phenomena result from beating of modes of the quantized cavity field that are not nearest neighbors. These beats can show up in the dynamics because in the strongly sub-Poissonian field there are only a few modes populated enough to effectively take part in the dynamics. Consequently, it is very unlikely that constructive interference between *any* pair of these populated modes is overcome by destructive interference between a multitude of modes with irregular phase differences. We have also shown that apart from the fractional revivals and "standard" revivals with ever-decreasing amplitudes, at certain times revivals with amplitudes very close to the original one appear; we call these revivals superrevivals, or revivals of the revivals, and the mechanism responsible for them is essentially the same as that responsible for fractional revivals. Overall, the very-long-time behavior of the sub-Poissonian JC model is dominated by spectacular and persistent superstructures. These superstructures resemble also superstructures reported for a nonlinear generalization of the JC model [8].

It has always been stated that the revivals can appear only if the initial number of photons is sufficiently large ($\bar{n} \sim 10$). We show in the present paper that this statement is not always correct. In particular, a detuning between the field and the atom "linearizes" the Rabi frequencies' spectrum and thus leads to distinct revivals. For long times, the revivals evolve into fractional revivals and superrevivals much as in the sub-Poissonian case, and we show in the present paper that the mechanism responsible for these superstructures is in both cases the same. It is very interesting that phenomena so far associated only with highly nonclassical states of the field can be in principle observed also in a coherent (classical) field. This is so because it is not the nonclassical nature of the sub-Poissonian field but rather the limited number of modes which effectively take part in the evolution and the rules of quantum interference that lead to fractional revivals and superrevivals.

It is to be stressed that long-time revivals were also studied in the context of the long-time behavior of atomic and molecular wave packets [9–12] (see also the review papers by Alber and Zoller [13] and Averbukh and Perelman [14]). In particular, these last authors presented a detailed discussion of fractional revivals in the time regime $t_{\rm cl} < t \ll t_R$, where $t_{\rm cl}$ is the period of the classical motion of the wave packet and t_R is the revival time. Another system in which the revivals were found is the

squeezed-quantum-kicked-rotator model [15].

This paper is organized as follows. In Sec. II we show the physical origin of the revivals that appear in the coherent JC model with a small number of photons and the atom and the field slightly detuned, and physical origin of various superstructures that appear in the long-time behavior of the model. In Sec. III we present approximate expressions for the quantum inversion, and in Sec. IV we discuss the envelope of the electric field associated with the oscillating dipole. We also show that these results cannot be obtained in the adiabatic approximation. We summarize our considerations in Sec. V.

II. REVIVALS WITH A SMALL NUMBER OF PHOTONS

A. Superstructures in the long-time behavior

Consider the JC model in the rotating-wave approximation (RWA). The Hamiltonian for the model reads

$$H = \tfrac{1}{2}\omega_0\sigma_3 + \omega a^\dagger a + g\left(a^\dagger\sigma^- + a\sigma^+\right) , \qquad (2.1)$$

where $a^\dagger$ and a are standard creation and annihilation operators for the harmonic oscillator, σ^+ and σ^- are spin raising and lowering operators, and g is the coupling constant. If we assume for simplicity that the atom is initially in its lower (unexcited) state, we obtain for the expectation value of σ_3, or the quantum inversion,

$$\langle\sigma_3(t)\rangle = C - W(t) = C - \sum_{n=1}^{\infty} P_n^2 B_n \cos\left(2\Lambda_n t\right) , \qquad (2.2)$$

where P_n^2 stands for the initial photon distribution,

$$B_n = \frac{ng^2}{\Lambda_n^2} , \qquad (2.3)$$

and the Rabi frequencies Λ_n are defined as

$$\Lambda_n = \sqrt{\tfrac{1}{4}\Delta^2 + ng^2}, \qquad (2.4)$$

with the detuning parameter $\Delta = \omega_0 - \omega$. The constant C is such that $\langle\sigma_3(0)\rangle = -1$.

It is very important that the detuning Δ and the coupling constant g should be small — otherwise the RWA cannot be properly applied. However, in all practical realizations of the Jaynes-Cummings model, the coupling constant is so small [2,4] that even detunings much larger than g are small enough for the RWA to be correct. To set a proper reference scale, in the following we will always set $\omega_0 = 1$ and $g = 10^{-6}$ corresponding to the experiment of Rempe *et al.* [4]. We list these quantities separately although only the values $\frac{g}{\omega_0}$, $\frac{g}{\Delta}$, and gt are relevant. To our knowledge the revivals have never been studied before in the context of detuning. However, the effect of interference between states of the quantized field that are not nearest was considered for a model [16] which is closely related to a nonresonant JC system.

If the initial field is coherent, P_n^2 is a Poissonian distribution. Authors who discussed the revivals usually set $\Delta = 0$. This simplifies calculations and resulting formulas, but as we will see, some interesting features of the model show up only if $\Delta \neq 0$. If the distribution is Poissonian with a mean number of photons $\bar{n}$, and if $\Delta = 0$, from Eq. (2.2) we get

$$W(t) = \sum_{n=1}^{\infty} \frac{\bar{n}^n}{n!} e^{-\bar{n}} \cos\left(2gt\sqrt{n}\right) . \qquad (2.5)$$

This formula is very well known. If $\bar{n}$ is large enough ($\bar{n} \sim 10$ or larger), well-formed revivals appear. They result from beating of all nearest-neighbor Rabi oscillators, which after an initial dephasing become in phase again. In particular, a revival occurs when the $\bar{n}$th and the $(\bar{n}+1)$th oscillators acquire a common phase. Some analytical approximations to the sum (2.5) have been proposed [5,17,18]; all of them apply to the saddle point method. However, this requires $\bar{n}$ to be large enough, and thus quantum revivals started to be associated with the saddle point method and large $\bar{n}$ expansions. It should, perhaps, be noted that the approximation proposed by Filipowicz in Ref. [17] is valid for $\bar{n}$ as small as 4, but it still relies on the saddle point method, applied in a more subtle manner, though. On the other hand, if $\bar{n}$ is small and the atom and the field are in resonance, no revivals appear. Instead, the quantum inversion exhibits a fairly irregular behavior.

Now we admit a detuning Δ such that $\Delta \ll \omega_0$ and

$$(g/\Delta)^2 \ll 1 . \qquad (2.6)$$

Figure 1(a) shows a plot of the inversion for an initial coherent state with $\bar{n} = 2$ and no detuning, and Fig. 1(b) shows a plot of the inversion with the same initial state of the field, but with a detuning satisfying the condition (2.6). One can see that for the resonant case the inversion behaves in a fairly irregular manner, while for

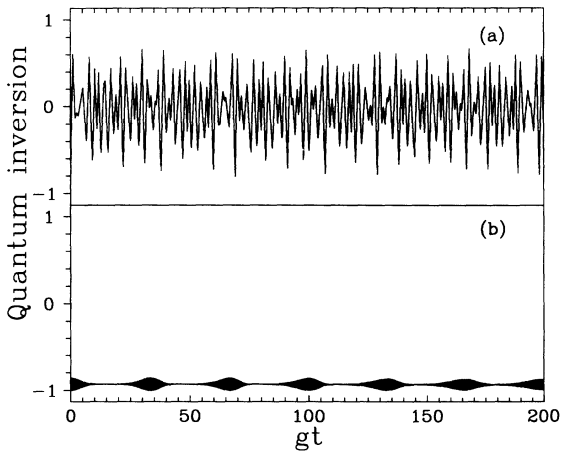

FIG. 1. Quantum inversion for the case of an initially coherent field with a small number of photons $\bar{n} = 2$ for (a) resonant ($\Delta = 0$) and (b) off-resonant ($\Delta = 10g$) cases. Other parameters are $\omega_0 = 1$, $g = 10^{-6}$. The atom is initially in its lower state.

the off-resonant case distinct revivals appear, each having a Gaussian envelope, much as they do in the large $\bar{n}$ case. Note though that the amplitudes of the revivals are very small.

If we compute the quantum inversion for longer times, the amplitudes of the consecutive revivals first decrease, but then they grow back to their original values — we may thus say that apart from the standard revivals there are "superrevivals," or revivals with amplitudes close to the original one. Note at this point that in the large $\bar{n}$ case the revivals' amplitudes always decrease until the individual revivals overlap and vanish altogether [5]. In the present case, the shape of the revivals also changes: they partially overlap to form complicated non-Gaussian objects but at times when the superrevival occurs almost regain their original Gaussian shape. This pattern repeats until the revivals eventually overlap at extremely long times. Overall, the long-time behavior of the model is dominated by very spectacular superstructures (cf. Fig. 2; from now on we plot only the time-dependent part of the inversion). These superstructures are very persistent: we observe distinct individual revivals and distorted, but still distinguishable superstructures for times as long as $gt \sim 10^6$.

B. Physical origin of the revivals

In order to understand the differences between the resonant and nonresonant cases, one should answer the following questions: why do the revivals appear in the latter and not appear in the former case, why are their amplitudes so small, what is the physical origin of the superstructures, and why do such superstructures not appear in the standard (coherent with $\bar{n}$ large) JC model?

The problem of amplitudes is straightforward: if $\Delta \neq 0$, the Rabi oscillations enter the sum in (2.2) with total factors which are products of the Poissonian factors P_n^2 and the weights B_n (2.3). The latter for small values of n are of order $4n(g/\Delta)^2$. The physical reason for the small amplitudes of the revivals is that if the atom and the field are detuned, the atom is reluctant to absorb a photon and tends to stay in the vicinity of its initial state.

The very existence of the revivals is much more fundamental. In the resonant case ($\Delta = 0$), the Rabi frequencies' spectrum is strongly nonlinear, while a detuning that satisfies the condition (2.6) linearizes it (cf. Fig. 3). If $\bar{n}$ is small, there are only a few modes populated enough to effectively take part in the evolution of the system. If the Rabi frequencies' spectrum is strongly nonlinear, differences between the neighboring modes vary greatly, and when one pair of these populated modes, say, $(\bar{n}+1)\leftrightarrow\bar{n}$, acquire a common phase and interfere constructively, other pairs, say, $\bar{n}\leftrightarrow(\bar{n}-1)$, interfere destructively and no revivals appear. Even at times when these two pairs do have a common phase, other pairs of modes with similar populations are out of phase and destructive interference prevails once more, and a very irregular behavior of the inversion results. On the other hand, it is obvious that if the Rabi frequencies' spectrum were linear, $\Lambda_n = \alpha + \beta n$, there would be an infinite series of ideal revivals, and it is *small* deviations from the linearity that produce both revivals for a limited range of times and changes in the revivals' amplitudes.

If $\bar{n}$ is large, the second derivative of Λ_n with respect to n taken at $n = \bar{n}$ is responsible for the decrease of the amplitudes and broadening of the consecutive revivals and their eventual overlapping. For $\bar{n}$ small this interpretation fails, which is most readily seen from the fact that in the present case the amplitudes first decrease, but then start to increase. We should therefore look for a more subtle explanation of the details of the long-time evolution of the system.

C. A measure of the overall phase difference

It is generally agreed that overlapping of the revivals results from accumulating of an overall phase difference between the beating modes. Before we can go any further, we should try to construct a measure of the accumulating phase "disorder." To this end we generalize a

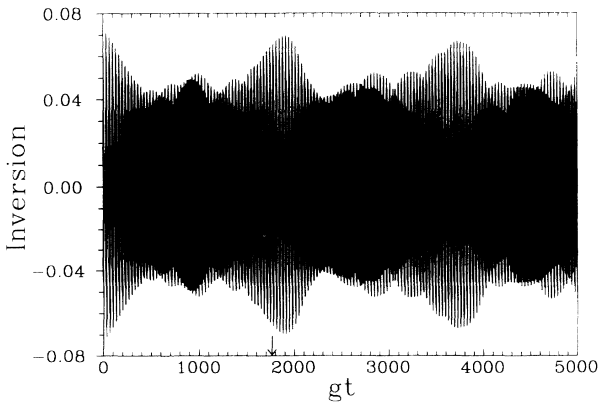

FIG. 2. A superstructure in the long-time behavior of the JC model. All parameters as in Fig. 1(b). Only the time-dependent part of the inversion is plotted. The arrow marks the position of the estimated "superrevival period" t_S given by (2.11).

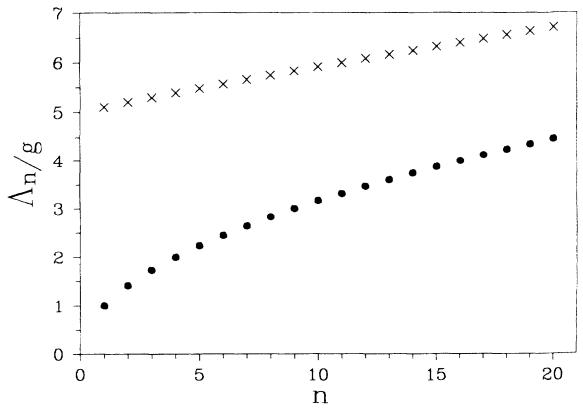

FIG. 3. Rabi frequencies for the resonant ($\Delta = 0$, bullets) and nonresonant ($\Delta = 10g$, crosses) JC models.

phase function $\varphi(t)$ that has been introduced in Ref. [7].

First, we want this phase function to be a continuous function of time. Therefore for each pair of beating modes we take their relative phase difference modulo 2π, and if the resulting number is less than π we take that number or 2π minus that number otherwise (note that phase differences equal to 0 or 2π both lead to a fully constructive interference). It seems also natural that a mode that does not bring an important contribution to the quantum inversion should not bring one to the "overall phase difference," either. We therefore multiply the contribution from each pair of beating modes by the product of total weights with which the corresponding terms enter the sum in (2.2). We thus arrive at

$$\varphi_{mn}(t) = \begin{cases} c\,P_m^2 P_n^2 B_m B_n x_{mn}\,, & x_{mn} < \pi \\ c\,P_m^2 P_n^2 B_m B_n (2\pi - x_{mn})\,, & x_{mn} > \pi\,, \end{cases}$$
$$x_{mn} = (2\Lambda_m t - 2\Lambda_n t) \bmod 2\pi\,, \tag{2.7}$$

$$\varphi(t) = \sum_{m=1}^{\infty} \sum_{n=1}^{m} \varphi_{mn}(t)\,, \tag{2.8}$$

where $\varphi(t)$ is the measure for the "overall phase difference," φ_{mn} is the contribution from the mth and nth pairs of modes, and c is a normalization constant. We choose c such that if all $\varphi_{mn} = \pi$ (fully destructive interference between each pair of modes), also $\varphi(t) = \pi$. Therefore

$$c = \left(\sum_{m=1}^{\infty} \sum_{n=1}^{m} P_m^2 P_n^2 B_m B_n \right)^{-1}. \tag{2.9}$$

In practice, $\varphi(t)$ never reaches π — except for the $t = 0$ there are always some modes which are in phase and some which are out of phase. For instance, when after the initial collapse the $\bar{n}$th and $(\bar{n}+1)$th modes have a phase difference of π, the $(\bar{n}+1)$th and $(\bar{n}-1)$th modes have, to a good approximation, a phase difference of 2π, etc.

It has been shown in Ref. [7] that the function (2.8) works fine for both the resonant coherent JC model with $\bar{n}$ large and for the resonant sub-Poissonian JC model. In either case, each individual revival is associated with a sharp minimum of $\varphi(t)$, and between revivals $\varphi(t)$ takes values around $\pi/2$. It should be noted that other measures of the accumulating "disorder" have been proposed (see, e.g., [19]), but the function (2.8) is very easy to calculate and behaves less irregularly around the revivals.

D. Physical origin of the superstructures

At $t = 0$, all modes are in phase and get out of phase for $t > 0$. The atomic inversion collapses, but at the time when the $(\bar{n}+1)$th and $\bar{n}$th modes acquire a phase difference of 2π, all other modes that are populated enough to matter have phase differences *approximately* equal to $2r\pi$ (r integer) and the first revival appears. The beating modes get out of phase again, and become in phase when the $(\bar{n}+1)$th and $\bar{n}$th modes acquire a phase difference of 4π, when the second revival appears. This time, however, phase differences between the other modes are less close to $2r'\pi$ (r' integer) and the second revival is smaller and broader than the first one. This situation is presented in Fig. 4, where the atomic inversion, the total phase function (2.8), and 12 most important contributions to the total phase function are plotted. As one can see, the first revival occurs when the nearest-neighbor contributions take their minima. For consecutive revivals, these minima no longer coincide, which results in broadening of the revivals, and the same holds for the higher-order neighbors' contributions. Each revival is associated with a pronounced minimum of the total phase function. The small minima of $\varphi(t)$ between the revivals can be associated with the minima of the third-neighbor contributions (or constructive interference between the third-order neighbors); the effect of constructive interference between the second-order neighbors in the middle of inter-revival periods is screened off by the fully destructive interference between the nearest neighbors.

As the system evolves, phase differences between neighboring pairs of modes become more and more important and destructive interference appears. In the large-$\bar{n}$ case this destructive interference eventually leads to the complete overlapping of the revivals. The situation is different in the small-$\bar{n}$ case, though. For some long times the phase difference between the $(\bar{n}+1)$th and $\bar{n}$th modes approaches a value of $2k\pi$ for some integer k, while the phase difference between the $\bar{n}$th and $(\bar{n}-1)$th modes approaches a value of $2(k+1)\pi$. Since there are very few populated modes and the Rabi frequencies' spectrum for these modes is *almost* linear, in this time domain phase differences between all these populated modes are *almost* equal to integer multiplications of 2π. As a result, constructive interference prevails once more, revivals regain their original amplitudes, and the superrevival appears. This situation is plotted in Fig. 5. Note that all important contributions to the phase function take their minima almost simultaneously.

We wish to stress that in the coherent large-$\bar{n}$ case it also happens that a couple of modes around the $\bar{n}$th one have relative phase differences which are simultaneously almost equal integer multiplications of 2π. However, as there are many more populated modes which for this specific time have phase differences far from 2π, constructive interference does not prevail and no superrevival, nor ordinary revival for that matter, can be seen. On the other hand, if $\bar{n}$ is large and the field distribution is very narrow (sub-Poissonian), superrevivals do occur and the mechanism that leads to them is precisely the same as in the present case [7].

We can estimate the "superrevival period" t_S as time for which

$$\begin{aligned} 2\Lambda_{\bar{n}+1} t_S - 2\Lambda_{\bar{n}} t_S &= 2k\pi\,, \\ 2\Lambda_{\bar{n}} t_S - 2\Lambda_{\bar{n}-1} t_S &= 2(k+1)\pi\,, \end{aligned} \tag{2.10}$$

for some integer k. Solving (2.10) for t_S we obtain

$$t_S = \frac{\pi}{2\Lambda_{\bar{n}} - \Lambda_{\bar{n}+1} - \Lambda_{\bar{n}-1}}\,. \tag{2.11}$$

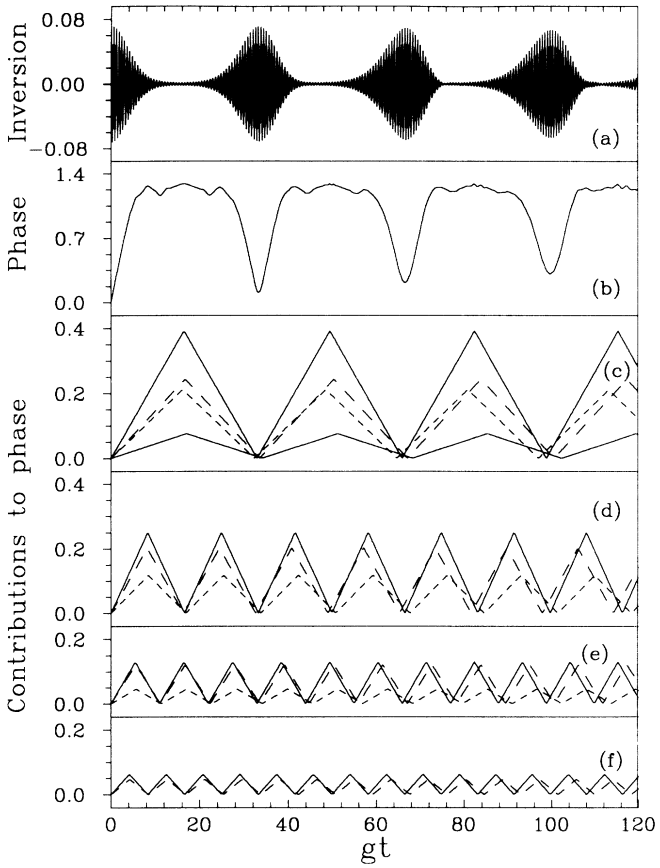

FIG. 4. Time-dependent part of the quantum inversion (a), total phase function $\varphi(t)$ (2.8), and (b) 12 most important contributions to $\varphi(t)$ (c)–(f) in the region of first revivals. (c) Nearest-neighbor contributions: $3\leftrightarrow2$ (solid line, large amplitude), $4\leftrightarrow3$ (long-dashed line), $2\leftrightarrow1$ (short-dashed line), $5\leftrightarrow4$ (solid line, small amplitude); (d) second-neighbor contributions: $4\leftrightarrow2$ (solid line), $3\leftrightarrow1$ (long-dashed line), $5\leftrightarrow3$ (short-dashed line); (e) third-neighbor contributions: $4\leftrightarrow1$ (solid line), $5\leftrightarrow2$ (long-dashed line), $6\leftrightarrow3$ (short-dashed line); (f) fourth-neighbor contributions: $5\leftrightarrow1$ (solid line), $6\leftrightarrow2$ (dashed line). The y-axis scale is kept the same in panels (c)–(f). All parameters as in Fig. 1(b).

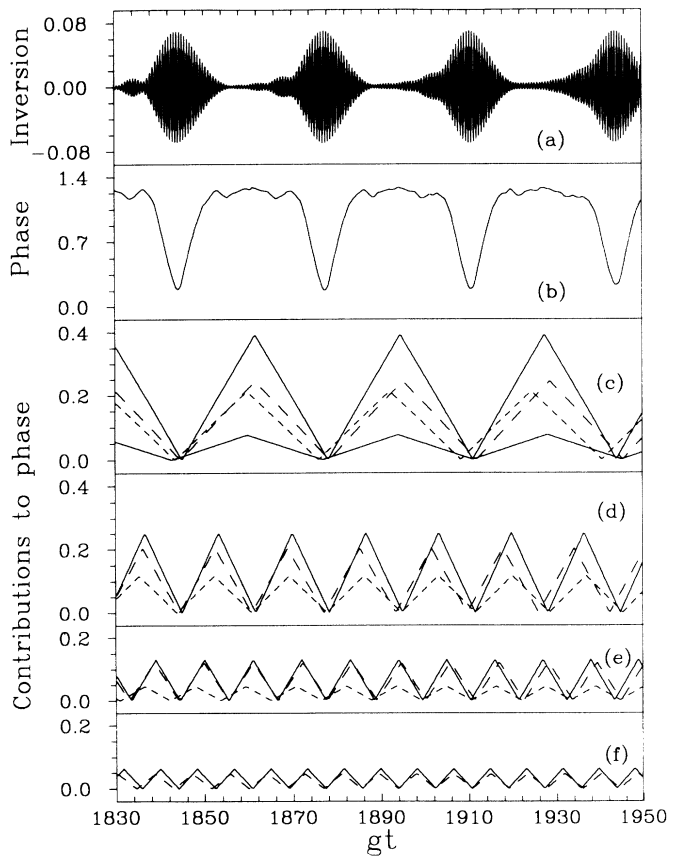

FIG. 5. Same as in Fig. 4, but in the region of superrevivals.

This t_S is marked by an arrow in Fig. 2. One can see that this is a qualitatively good result. Strictly speaking, (2.10) cannot be solved for an *integer* k — Rabi frequencies are in general irrational and incommensurate, and there is no exact periodicity in the system. This is also the reason for the expression (2.11) being only qualitatively good.

As the Rabi frequencies' spectrum is almost linear, phase differences between the second-order neighbors are approximately twice larger than between the nearest neighbors. Consider the most populated pairs of second-order neighbors. There are times when the phase difference between the $(\bar{n}+2)$th and $\bar{n}$th modes equals $2l\pi$ for some integer l, and the phase difference between the $(\bar{n}+1)$th and $(\bar{n}-1)$th modes equals $2(l+1)\pi$, while the nearest neighbors are neither simultaneously in phase nor out of phase. This is the region of the so-called fractional revivals [6,7] — distinct revivals form and follow each other two times faster than for the short times (see Fig. 6); if the original revival period is t_R, in this time domain the revival period is approximately $t_R/2$. This happens around $t_2 \simeq t_S/2$, and t_2 can be further approximated as

$$2\Lambda_{\bar{n}+2}t_2 - 2\Lambda_{\bar{n}}t_2 = 2l\pi\,, \tag{2.12}$$

$$2\Lambda_{\bar{n}+1}t_2 - 2\Lambda_{\bar{n}-1}t_2 = 2(l+1)\pi\,, \tag{2.13}$$

from which we get

$$t_2 = \frac{\pi}{\Lambda_{\bar{n}+1} - \Lambda_{\bar{n}+2} - \Lambda_{\bar{n}-1} + \Lambda_{\bar{n}}}\,. \tag{2.14}$$

Again, (2.12) cannot be solved for integer l and this t_2 is only qualitatively good.

A very similar situation occurs when the third neighbors are simultaneously in phase, while phase differences between the nearest and second neighbors take intermediate values (Fig. 7). Distinct revivals form, although their separation is worse than in any of the cases discussed above. In these time domains revivals follow each other three times faster than for initial times. Note that each revival is also reinforced by constructive interference between one of the three most populated pairs of nearest neighbors. A qualitatively good approximation to the time when the period $t_R/3$ fractional revivals appear can be derived in a manner similar to (2.12). Note that this type of fractional revivals appears twice within the same "superrevival period," namely, around $t \simeq t_S/3$ and $t \simeq 2t_S/3$.

As a matter of principle, one could also expect higher-order fractional revivals to appear. For instance, in the sub-Poissonian case, distinct period $t_R/4$ fractional revivals appear around $t \simeq t_S/4$ [7]. This type of fractional revivals occurs when the fourth neighbors become in phase, while the phase differences between the nearest, second, and third neighbors take intermediate values. However, in the present case contributions from the

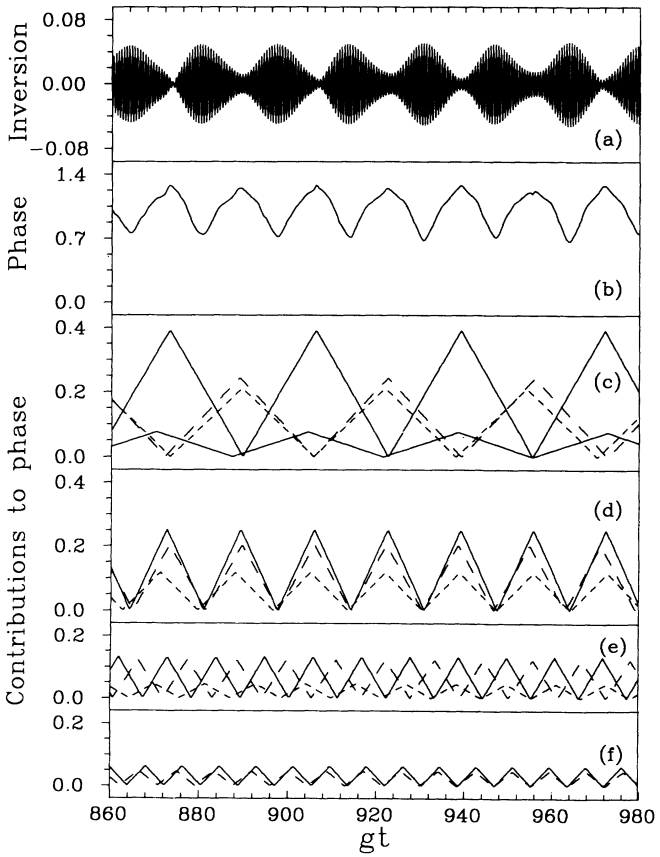

FIG. 6. Same as in Fig. 4, but in the region of period $t_R/2$ fractional revivals.

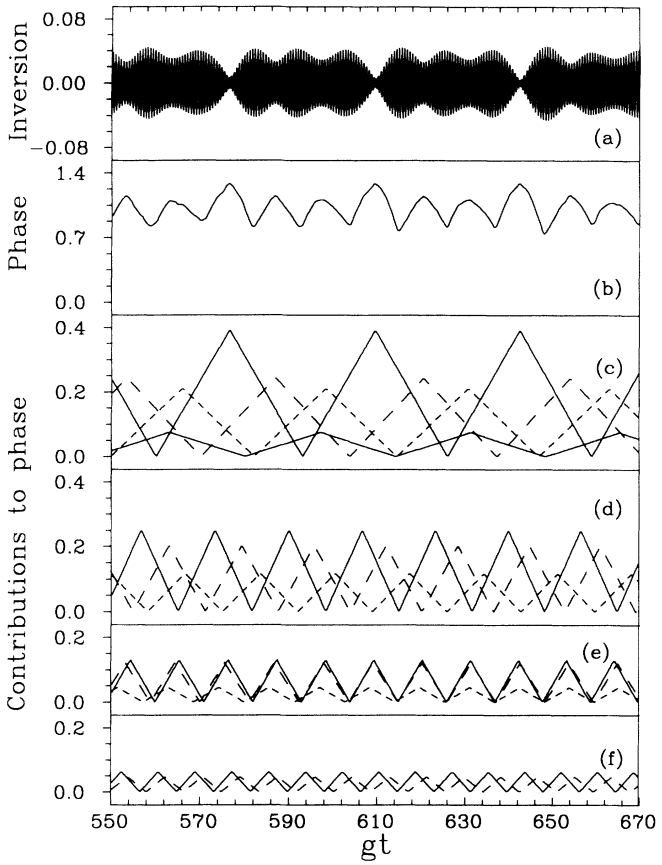

FIG. 7. Same as in Fig. 4, but in the region of period $t_R/3$ fractional revivals.

fourth neighbors enter the sum in (2.2) with such small weights that their constructive interference is overcome by destructive interference between the nearest neighbors. As a result, around $t \simeq t_S/4$ and $t \simeq 3t_S/4$ one can see broad bands of Rabi nutations with poorly separated peaks.

For $t > t_S$ the whole pattern repeats, although the details are blurred. Nevertheless, the superstructures that we have just described are very persistent: we see individual well separated revivals and distorted superstructures for times as long as $gt \sim 10^6$.

If the detuning is larger than $10g$, the superstructures are even more persistent and the "superstructure period" becomes very large. These observations are easy to explain: the larger Δ, the smaller the deviations from the linearity in the Rabi frequencies' spectrum and the beating modes must take more time to get out of phase and then back in phase again. Also our approximations (2.11) and (2.14) give better results. However, as Δ increases, the amplitudes of the revivals decrease.

III. APPROXIMATE EXPRESSIONS FOR THE INVERSION

If $\bar{n}$ is small and the detuning satisfies the condition (2.6), Rabi frequencies (2.4) can be expanded as

$$\Lambda_n = \tfrac{1}{2}\Delta + n\Delta(g/\Delta)^2 - n^2\Delta(g/\Delta)^4 + \cdots . \tag{3.1}$$

We stress that this expansion makes sense only if $\bar{n}$ is small: for large n the "corrections" might dominate the leading term. However, if $\bar{n}$ is small, the Poissonian distribution is very narrow and terms with badly approximated frequencies do not bring important contribution to the sum in (2.2). Similarly, the weights (2.3) can be expanded as

$$B_n = 4n(g/\Delta)^2 - 16n^2(g/\Delta)^4 + \cdots . \tag{3.2}$$

If we keep terms to the order $(g/\Delta)^2$ in (3.1) and (3.2), from (2.2) we obtain for the time-dependent part of the inversion

$$W(t) \approx 4\bar{n}(g/\Delta)^2 \exp\left\{-\bar{n}\left[1-\cos 2\Delta(g/\Delta)^2 t\right]\right\} \cos\left[\Delta t + 2\Delta(g/\Delta)^2 t + \bar{n}\sin 2\Delta(g/\Delta)^2 t\right] . \tag{3.3}$$

One can see that (3.3) describes an infinite series of perfect revivals. No superstructure or any overlapping of the revivals can be seen. Similar results can be obtained without expanding the weights B_n in a power series in $(g/\Delta)^2$, but then the resulting sum cannot be evaluated analytically. It shows that the simple assumption of the Rabi frequencies spectrum being linear leads to (perfect) revivals even for a small-$\bar{n}$ case, contrary to a common view that in such a situation no distinct revivals can appear.

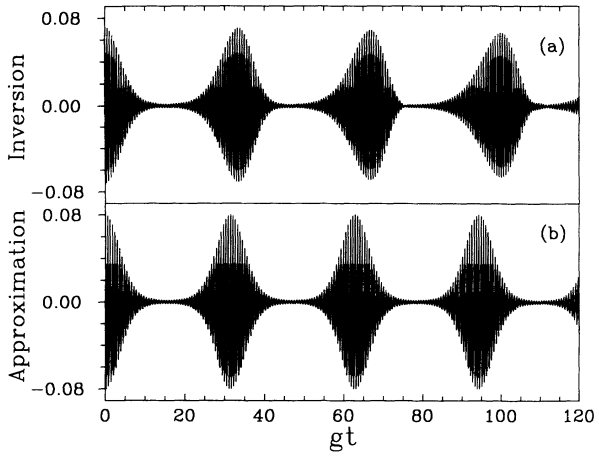

FIG. 8. Time-dependent part of the exact atomic inversion (a) and the second-order approximation (3.3) (b) in the region of first revivals. All parameters as in Fig. 1(b).

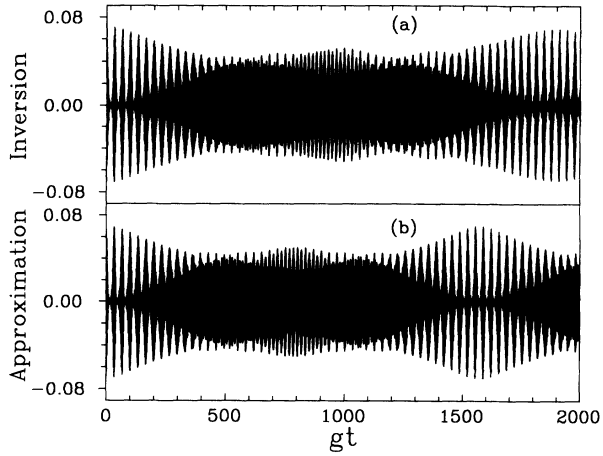

FIG. 9. Time-dependent part of the exact atomic inversion (a) and the fourth-order approximation (b). The region corresponding to the first "superrevival period" of the exact inversion is shown. All parameters as in Fig. 1(b).

For the detuning $\Delta = 10g$ the approximation (3.3) gives qualitatively good results for a couple of first revivals (Fig. 8). The agreement is even better for larger detunings, but, as we have mentioned, with larger detunings the amplitudes of the revivals become very small.

Note that the approximation (3.3) contains terms of order higher than $(g/\Delta)^2$ hidden in the sine and cosine functions (cf. [20]). However, we have not attempted to construct a second-order expression for the inversion. Instead, we have *independently* expanded Λ_n and B_n in powers of (g/Δ), and as one can see, such a procedure leads to qualitatively good results for small times. The strictly second-order expression for the inversion is

$$W(t) \approx 4\bar{n}(g/\Delta)^2 \cos \Delta t \,. \tag{3.4}$$

Equation (3.4) might be obtained directly from (2.2) by expanding the latter in powers of (g/Δ) or by using general formulas of Ref. [20] for the adiabatic approximation to the JC model. The adiabatic inversion (3.4) is purely oscillatory and does not exhibit any revivals.

If we keep terms of order $(g/\Delta)^4$ in the expansions of Λ_n and B_n, the agreement between the approximation and the actual inversion is almost perfect for a couple of first revivals, and for longer times we obtain a clear superstructure (Fig. 9). However, this approximated superstructure has a shorter "superrevival period," which shows that, at least for so small a detuning ($\Delta = 10g$), terms of order higher than $(g/\Delta)^4$ also play an important role.

If we expand the denominator of the "superrevival period" t_S given by (2.11) in powers of (g/Δ), we notice that the first nonvanishing term is proportional to $(g/\Delta)^4$:

$$t_S \approx \frac{\pi}{2\Delta(g/\Delta)^4} \,. \tag{3.5}$$

It is now clear why the "superrevival period" increases rapidly with decreasing ratio of $(g/\Delta)^2$. The equation (3.5) is consistent with the observation that a superstructure appears only in the fourth-order expansion of the Rabi frequencies.

IV. ENVELOPE OF THE ELECTRIC FIELD

Already Narozhny and his collaborators [5] observed that real and imaginary parts of the complex envelope of the electric field associated with the oscillating atomic dipole

$$D^+(t) = \langle \sigma^+(t) e^{-i\omega t} \rangle \tag{4.1}$$

exhibit revival-like behavior. What is perhaps also interesting is that this complex envelope can be divided into slow and fast components, and the slow parts oscillate with a period equal to twice the revival period. The same holds true for the present case. After some trivial algebra we get

$$D^+(t) = ig\sqrt{\bar{n}} \sum_{n=0}^{\infty} \frac{\bar{n}^n}{n!} e^{-\bar{n}} \sin \Lambda_{n+1} t \left(\frac{1}{\Lambda_{n+1}} \cos \Lambda_n t + i \frac{\Delta/2}{\Lambda_n \Lambda_{n+1}} \sin \Lambda_n t \right) , \tag{4.2}$$

and the slow and fast components are

$$
\begin{aligned}
\mathrm{Re}\, D^+(t)_{\mathrm{slow}} &= -\tfrac{1}{2} g\sqrt{\bar{n}} \sum_{n=0}^{\infty} \frac{\bar{n}^n}{n!} e^{-\bar{n}} \frac{\Delta/2}{\Lambda_n \Lambda_{n+1}} \cos(\Lambda_{n+1} - \Lambda_n) t\,, \\
\mathrm{Re}\, D^+(t)_{\mathrm{fast}} &= \tfrac{1}{2} g\sqrt{\bar{n}} \sum_{n=0}^{\infty} \frac{\bar{n}^n}{n!} e^{-\bar{n}} \frac{\Delta/2}{\Lambda_n \Lambda_{n+1}} \cos(\Lambda_{n+1} + \Lambda_n) t\,, \\
\mathrm{Im}\, D^+(t)_{\mathrm{slow}} &= \tfrac{1}{2} g\sqrt{\bar{n}} \sum_{n=0}^{\infty} \frac{\bar{n}^n}{n!} e^{-\bar{n}} \frac{1}{\Lambda_{n+1}} \sin(\Lambda_{n+1} - \Lambda_n) t\,, \\
\mathrm{Im}\, D^+(t)_{\mathrm{fast}} &= \tfrac{1}{2} g\sqrt{\bar{n}} \sum_{n=0}^{\infty} \frac{\bar{n}^n}{n!} e^{-\bar{n}} \frac{1}{\Lambda_{n+1}} \sin(\Lambda_{n+1} + \Lambda_n) t\,.
\end{aligned}
\tag{4.3}
$$

The components (4.3) are plotted in Fig. 10. The fast components indeed display a revival-like behavior, while the slow parts oscillate with a period equal to twice the revival period. For longer times, the complex electric field envelope displays a distinct superstructure (Fig. 11). Note that while the superstructures of the fast components mimic that of the inversion, the "superstructure period" of the slow components is twice as large as the "superrevival period."

To calculate the complex electric field envelope in the adiabatic approximation, we use formulas of Ref. [20] for $\sigma^+(t)$ in this approximation. We obtain for the slow and fast components

$$
\begin{aligned}
\mathrm{Re}\, D^+(t)_{\mathrm{slow}} &= -\frac{g\sqrt{\bar{n}}}{\Delta}\,, \\
\mathrm{Re}\, D^+(t)_{\mathrm{fast}} &= \frac{g\sqrt{\bar{n}}}{\Delta} \cos \Delta t\,, \\
\mathrm{Im}\, D^+(t)_{\mathrm{slow}} &= 0\,, \\
\mathrm{Im}\, D^+(t)_{\mathrm{fast}} &= \frac{g\sqrt{\bar{n}}}{\Delta} \sin \Delta t\,.
\end{aligned}
\tag{4.4}
$$

One can see that in the adiabatic approximation the fast components display unmodulated oscillations, while the slow components remain constant. This is in full agreement with our previous observation that the quantum inversion does not display any revivals in this approx-

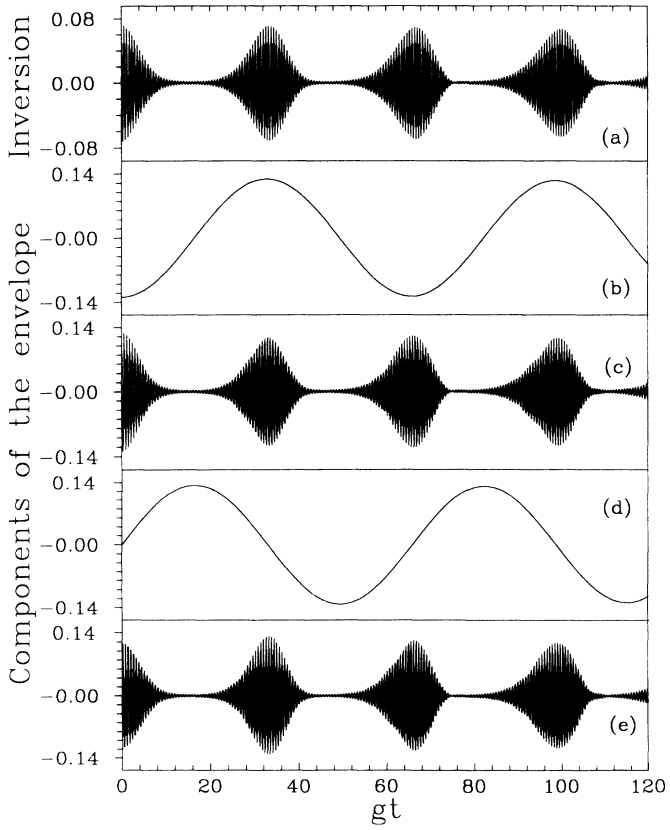

FIG. 10. Time-dependent part of the quantum inversion (a) and components of the envelope of the electric field associated with the atomic dipole (b)–(e) in the region of first revivals. (b) Slow component of the real part of the envelope, (c) fast component of the real part of the envelope, (d) slow component of the imaginary part, (e) fast component of the imaginary part. All parameters as in Fig. 1(b).

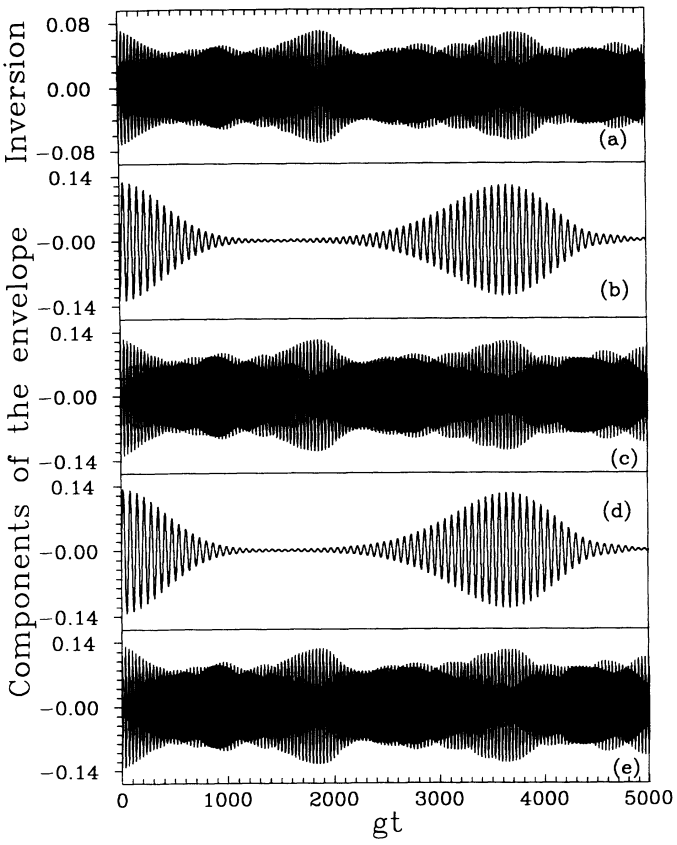

FIG. 11. Same as in Fig. 10 but for long times.

imation [cf. Eq. (3.4)]. However, if all frequencies and coefficients in (4.3) are replaced by their lowest-order expansions, we obtain

$$
\begin{aligned}
\mathrm{Re}\, D^{+}(t)_{\mathrm{slow}} &= -\frac{g\sqrt{\bar{n}}}{\Delta}\cos[\Delta(g/\Delta)^2 t]\,, \\
\mathrm{Re}\, D^{+}(t)_{\mathrm{fast}} &= \frac{g\sqrt{\bar{n}}}{\Delta}\exp\left\{-\bar{n}\left[1-\cos 2\Delta(g/\Delta)^2 t\right]\right\}\cos\left\{\Delta t+\Delta(g/\Delta)^2 t+\bar{n}\sin[2\Delta(g/\Delta)^2 t]\right\}\,, \\
\mathrm{Im}\, D^{+}(t)_{\mathrm{slow}} &= \frac{g\sqrt{\bar{n}}}{\Delta}\sin[\Delta(g/\Delta)^2 t]\,, \\
\mathrm{Im}\, D^{+}(t)_{\mathrm{fast}} &= \frac{g\sqrt{\bar{n}}}{\Delta}\exp\left\{-\bar{n}\left[1-\cos 2\Delta(g/\Delta)^2 t\right]\right\}\sin\left\{\Delta t+\Delta(g/\Delta)^2 t+\bar{n}\sin[2\Delta(g/\Delta)^2 t]\right\}\,.
\end{aligned}
\tag{4.5}
$$

The approximation (4.5) contains terms of order higher than second in $(g/\Delta)^2$. Nevertheless, in this approximation the fast components display revival-like behavior with a revival period equal to the quantum inversion revival period in the approximation (3.3), and the slow components oscillate with half that frequency. The approximation (4.5) does not give any superstructures in the long-time behavior, but it gives qualitatively good results in the short-time (single revival) scale, much as the approximation (3.3) for the quantum inversion does. Our approximation scheme, independent expanding of frequencies and coefficients, gives accurate results at least in the short-time scale, while a "correct" second-order approximation does not describe revivals either in the inversion, or in the complex electric field envelope.

V. SUMMARY AND CONCLUSIONS

We have shown in the present paper that in the JC model with the field prepared initially in a coherent state with a small average number of photons $\bar{n}$, the quantum inversion displays distinct collapses and revivals provided the atom and the field are slightly detuned. This is a consequence of the fact that the detuning linearizes the Rabi frequencies' spectrum and makes the phase differences between the few modes that effectively take part in the dynamics of the system less irregular than in the resonant case. In addition, long-time behavior of the model is dominated by very spectacular superstructures: fractional revivals and superrevivals (which, incidentally, might be thought of as period t_R fractional revivals), de-

scribed in the context of the JC model with a strongly sub-Poissonian field distribution. The fractional revivals result from constructive interference between some pairs of beating modes of the quantized field, but not the pairs of the nearest neighbors, which was the case for the standard revivals, but rather pairs of second or third neighbors. In our opinion, this phenomenon demonstrates the "granularity," or the quantum nature, of the field even more strongly than the standard revivals do. It is very interesting that such fractional revivals can appear also if the initial field is coherent (classical), because as they do not require a strongly squeezed radiation on input, they should be in principle easier to observe in the laboratory.

We have also shown that the envelope of the electric field associated with the oscillating atomic dipole can be divided into slowly and quickly varying components. Both types of components also display clear long-time superstructures, but the "superstructure period" of the slow components is twice as large as the "superrevival period" of the quantum inversion. This observation supports the statement that when the atom completes one cycle of its evolution, the field completes only a half of its cycle — not only in the short-time (single revival), but also in the long-time (superrevival) scale.

Finally, we have demonstrated that these results cannot be obtained in the strictly second-order (adiabatic) approximation: this approximation leads to a purely oscillatory behavior of the quantities of interest, with no superstructures or even revivals. However, if the Rabi frequencies and the coefficients are *independently* expanded in powers of $(g/\Delta)^2$, more accurate approximations are obtained: the lowest order [terms up to $(g/\Delta)^2$] gives an infinite series of perfect revivals, and higher orders describe the long-time superstructures.

As for the possibility of observing superrevivals, they are beyond current experiments on cavity QED, due to short interaction time. In order to observe long-time fractional revivals the interaction time should be increased by a factor 3–10. An additional order of magnitude is needed for the nonresonant effects of the present paper. However, the study can be considered as a proposal for future experiments on cavity QED. The analysis presented in this work has also the potential to be applied in other atomic and molecular experiments outside the restrictive experimental environment of a micromaser.

ACKNOWLEDGMENTS

We would like to thank Professor Kazimierz Rzążewski for many stimulating discussions and comments. This work has been partially supported by Curie Joint Fund II under Grant No. MEN/NSF/92-116, and by Polish KBN Grant No. PB 2603/2.

[1] E. T. Jaynes and F. W. Cummings, Proc. IEEE **51**, 89 (1963).

[2] P. Goy, J. D. Raimond, M. Gross, and S. Haroche, Phys. Rev. Lett. **50**, 1903 (1983); I. Moi, P. Goy, M. Gross, J. D. Raimond, C. Fabre, and S. Haroche, Phys. Rev. A **27**, 2043 (1983); P. Filipowicz, P. Meystre, G. Rempe, and H. Walther, Opt. Acta **32**, 1105 (1985); P. L. Knight, in *Frontiers in Quantum Optics*, edited by E. R. Pike and Sarben Sarkar (Hilger, Bristol, 1986); H. Walther, At. Phys. **10**, 333 (1987), and references quoted therein.

[3] D. Meschede, H. Walther, and G. Müller, Phys. Rev. Lett. **54**, 551 (1985).

[4] G. Rempe, H. Walther, and N. Klein, Phys. Rev. Lett. **58**, 353 (1987).

[5] J. H. Eberly, N. B. Narozhny, and J. J. Sanchez-Mondragon, Phys. Rev. Lett. **44**, 1323 (1980); N. B. Narozhny, J. J. Sanchez-Mondragon, and J. H. Eberly, Phys. Rev. A **23**, 236 (1981); H.-I. Yoo and J. H. Eberly, Phys. Rep. **118**, 239 (1985).

[6] I. Sh. Averbukh and N. F. Perelman, Phys. Lett. A **139**, 449 (1989); I. Sh. Averbukh, Phys. Rev. A **46**, 2205 (1992).

[7] P. F. Góra and C. Jedrzejek, Phys. Rev. A **48**, 3291 (1993).

[8] J. Seke and F. Rattay, Phys. Rev. A **39**, 171 (1989); V. Bužek and I. Jex, Opt. Commun. **78**, 425 (1990); M. J. Werner and H. Risken, Phys. Rev. A **44**, 4623 (1991); P. Góra and C. Jedrzejek, *ibid.* **45**, 6816 (1992); A. Miranowicz, W. Tanaś, and S. Kielich, Quantum Opt. **2**, 253 (1990).

[9] J. Parker and C. R. Stroud, Phys. Rev. Lett. **56**, 716 (1986); J. A. Yeazell, M. Mallalieu, and C. R. Stroud, *ibid.* **64**, 2007 (1990).

[10] M. Nauenberg, J. Phys. B **23**, L385 (1990).

[11] M. Gruebele and A. H. Zewail, J. Chem. Phys. **98**, 883 (1993).

[12] T. Baumert, V. Engel, C. Rottgermann, W. T. Strunz, and G. Gerber, Chem. Phys. Lett. **191**, 639 (1992).

[13] G. Alber and P. Zoller, Phys. Rep. **199**, 231 (1991).

[14] I. Sh. Averbukh and N. F. Perelman, Usp. Fiz. Nauk **161**, 41 (1991) [Sov. Phys. Usp. **34**, 572 (1991)].

[15] K. Życzkowski, J. Phys. A **22**, L1147 (1989).

[16] B. Yurke and D. Stoler, Phys. Rev. Lett. **57**, 13 (1986).

[17] P. Filipowicz, J. Phys. A **19**, 3785 (1986); J. I. Cirac and L. L. Sánchez-Soto, Phys. Rev. A **40**, 3743 (1989).

[18] M. Venkata Satyanarayana, P. Rice, Reeta Vyas, and H. J. Carmichael, J. Opt. Soc. Am. B **6**, 228 (1989).

[19] S. J. D. Phoenix and P. L. Knight, Ann. Phys. (N.Y.) **186**, 381 (1988); Phys. Rev. Lett. **66**, 2833 (1991); Phys. Rev. A **44**, 6032 (1991); V. Bužek, H. Moya-Cessa, P. L. Knight, and S. J. D. Phoenix, *ibid.* **45**, 8190 (1992).

[20] J. R. Ackerhalt and K. Rzążewski, Phys. Rev. A **12**, 2549 (1975).

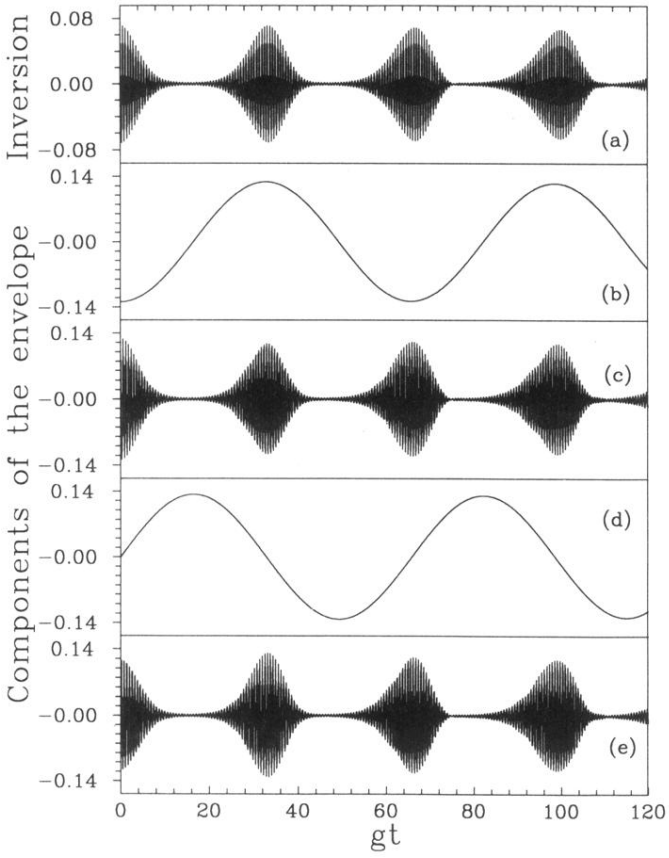

FIG. 10. Time-dependent part of the quantum inversion (a) and components of the envelope of the electric field associated with the atomic dipole (b)–(e) in the region of first revivals. (b) Slow component of the real part of the envelope, (c) fast component of the real part of the envelope, (d) slow component of the imaginary part, (e) fast component of the imaginary part. All parameters as in Fig. 1(b).

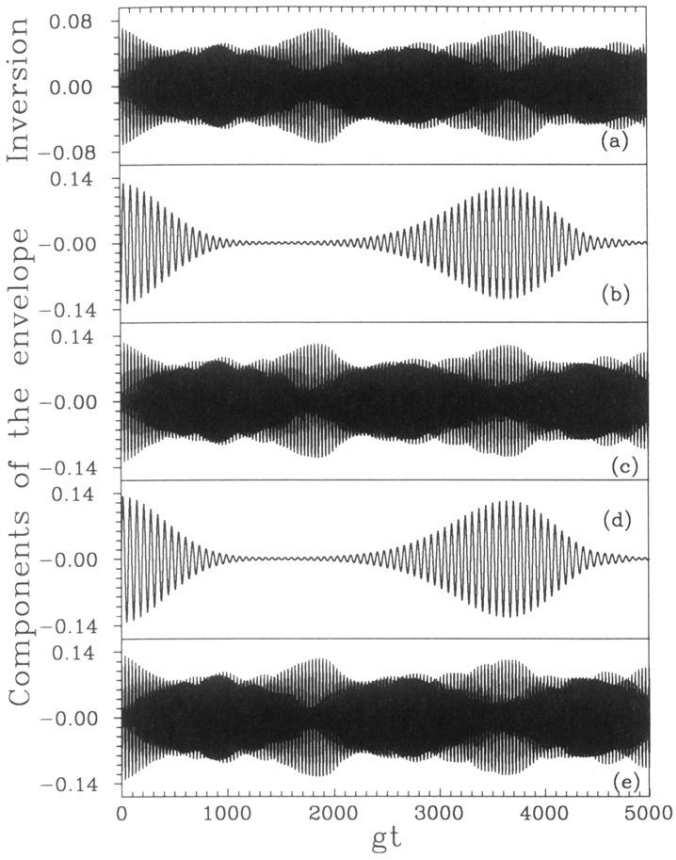

FIG. 11. Same as in Fig. 10 but for long times.

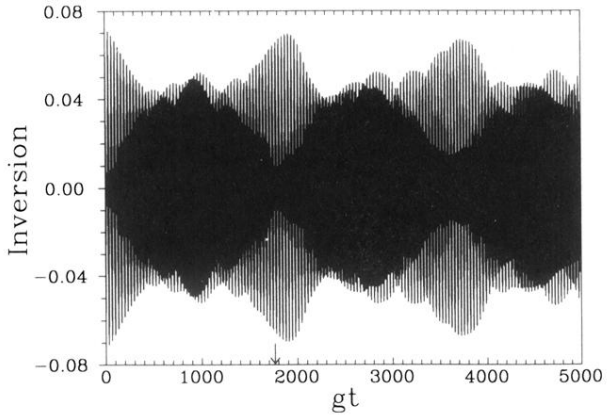

FIG. 2. A superstructure in the long-time behavior of the JC model. All parameters as in Fig. 1(b). Only the time-dependent part of the inversion is plotted. The arrow marks the position of the estimated "superrevival period" t_S given by (2.11).

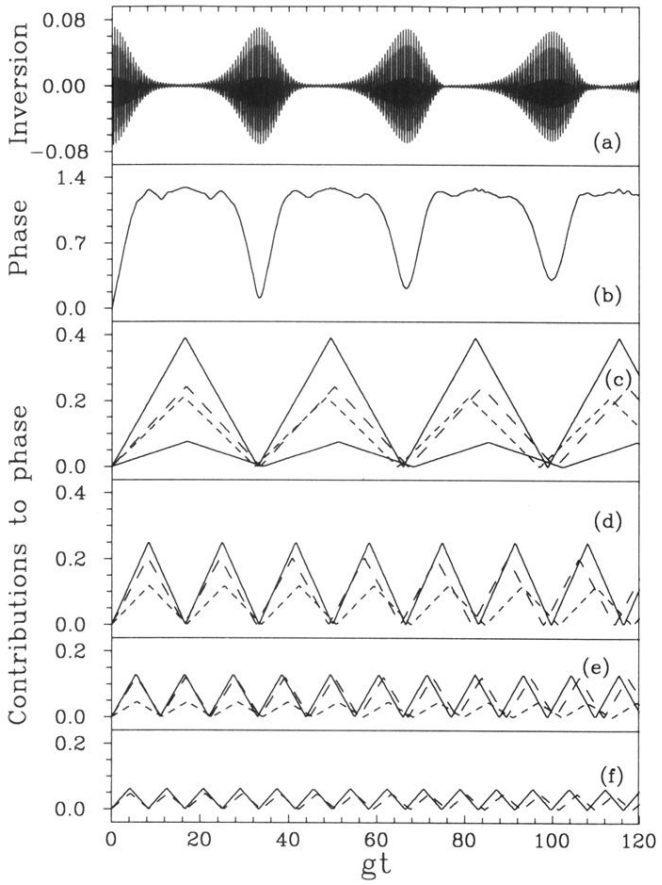

FIG. 4. Time-dependent part of the quantum inversion (a), total phase function $\varphi(t)$ (2.8), and (b) 12 most important contributions to $\varphi(t)$ (c)–(f) in the region of first revivals. (c) Nearest-neighbor contributions: $3\leftrightarrow2$ (solid line, large amplitude), $4\leftrightarrow3$ (long-dashed line), $2\leftrightarrow1$ (short-dashed line), $5\leftrightarrow4$ (solid line, small amplitude); (d) second-neighbor contributions: $4\leftrightarrow2$ (solid line), $3\leftrightarrow1$ (long-dashed line), $5\leftrightarrow3$ (short-dashed line); (e) third-neighbor contributions: $4\leftrightarrow1$ (solid line), $5\leftrightarrow2$ (long-dashed line), $6\leftrightarrow3$ (short-dashed line); (f) fourth-neighbor contributions: $5\leftrightarrow1$ (solid line), $6\leftrightarrow2$ (dashed line). The y-axis scale is kept the same in panels (c)–(f). All parameters as in Fig. 1(b).

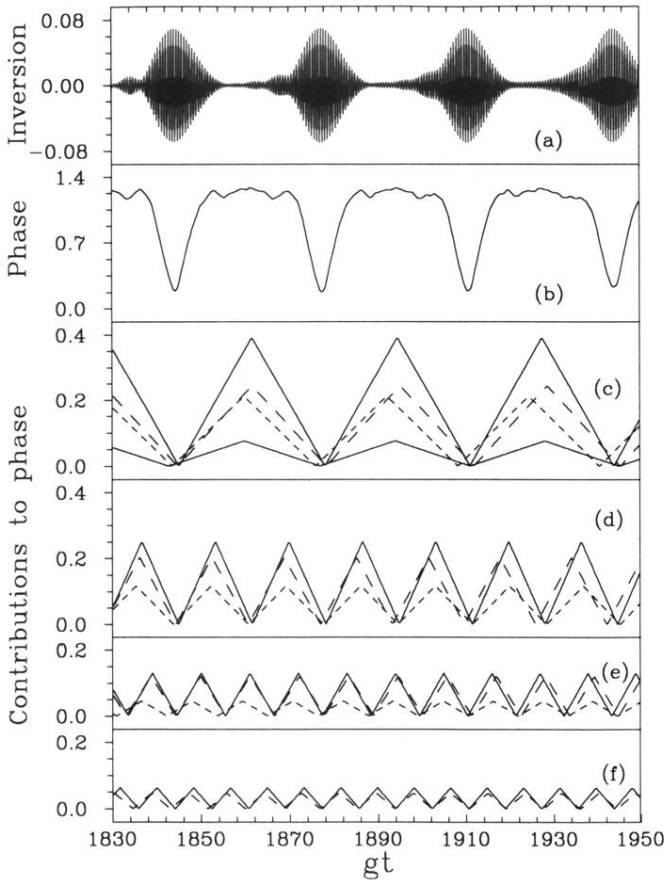

FIG. 5. Same as in Fig. 4, but in the region of superrevivals.

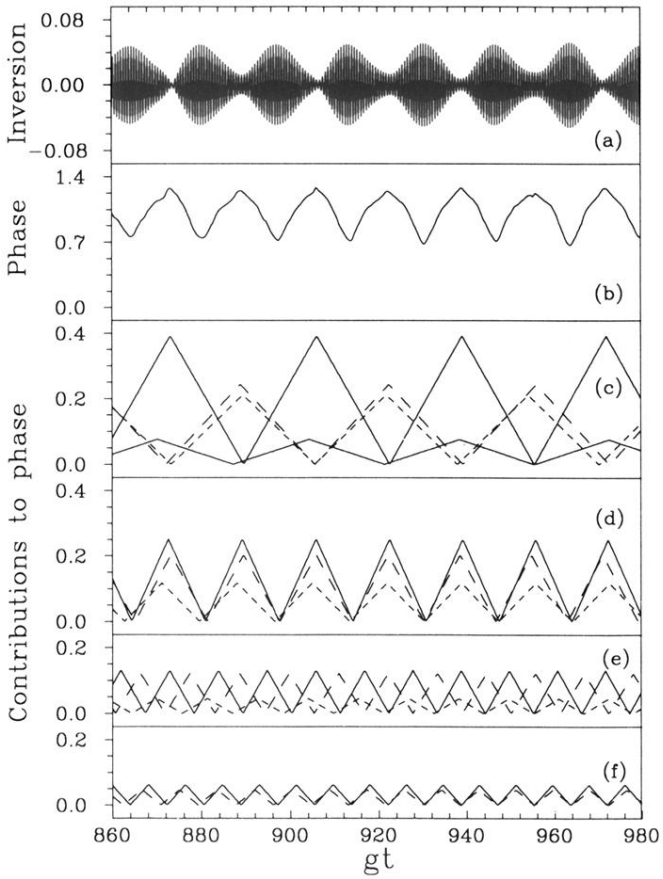

FIG. 6. Same as in Fig. 4, but in the region of period $t_R/2$ fractional revivals.

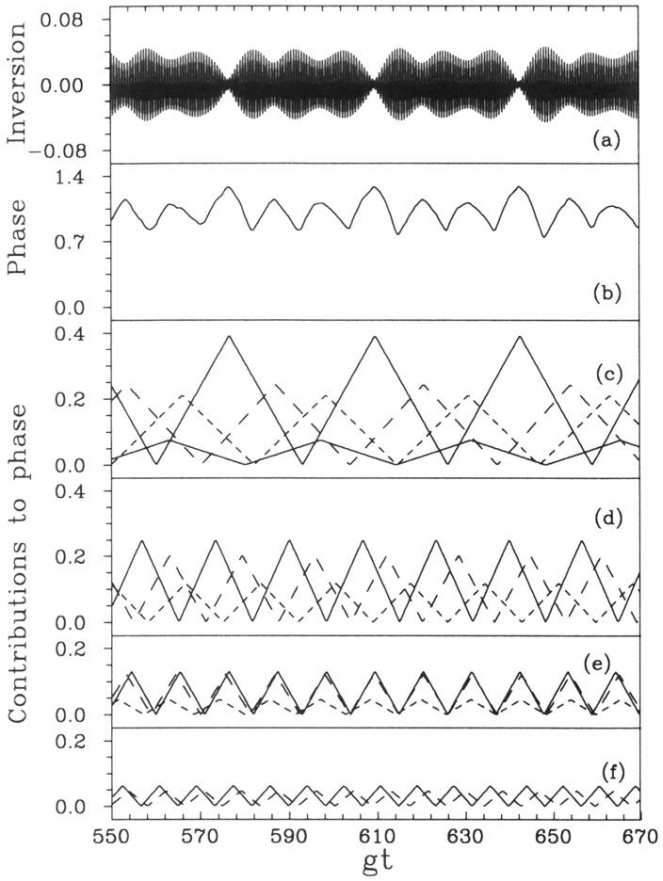

FIG. 7. Same as in Fig. 4, but in the region of period $t_R/3$ fractional revivals.

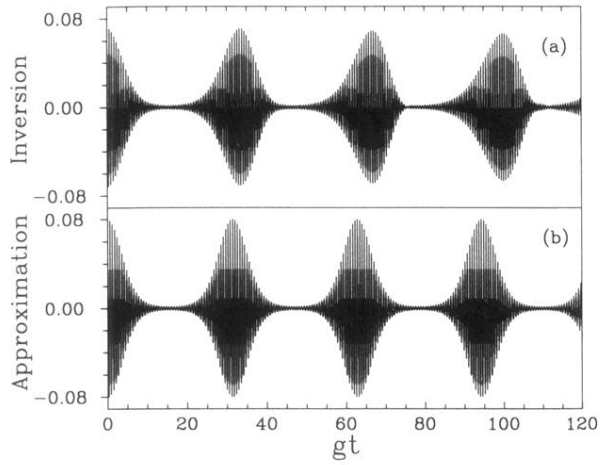

FIG. 8. Time-dependent part of the exact atomic inversion (a) and the second-order approximation (3.3) (b) in the region of first revivals. All parameters as in Fig. 1(b).

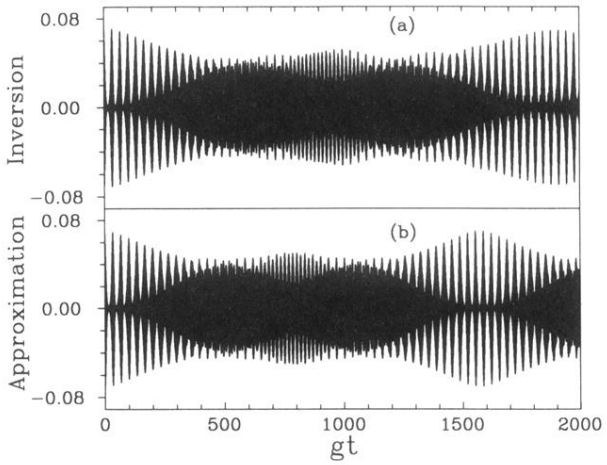

FIG. 9. Time-dependent part of the exact atomic inversion (a) and the fourth-order approximation (b). The region corresponding to the first "superrevival period" of the exact inversion is shown. All parameters as in Fig. 1(b).